J. Biochem. 126, 200-211 (1999)

Calcium-Induced Changes in the Location and Conformation of Troponin in Skeletal Muscle Thin Filaments[1]

Takashi Ishikawa*,[2] and Takeyuki Wakabayashi†,[3]

Photosynthesis Research Laboratory, the Institute of Physical and Chemical Research (RIKEN), 2-1, Wako, Saitama; and †Department of Physics, School of Science, University of Tokyo, 7-3-1, Hongo, Bunkyo-ku, Tokyo 113-0033

Received February 9, 1999; accepted May 6, 1999

Troponin is the regulatory protein of striated muscle. Without Ca^{2+}, the contraction of striated muscle is inhibited. Binding of Ca^{2+} to troponin activates contraction. The location of troponin on the thin filaments and its relation to the regulatory mechanism has been unknown, though the Ca^{2+}-induced dislocation of tropomyosin has been studied. By binding troponin(C+I) to actin in an almost stoichiometric ratio and reconstituting actin-tropomyosin-troponin(C+I) filaments, we reconstructed the three-dimensional structure of actin-tropomyosin-troponin(C+I) *with* or *without* Ca^{2+} from electron cryomicrographs to about 2.5 or 3 nm resolution, respectively. *Without* Ca^{2+}, the three-dimensional map reveals the extra-density region due to troponin(C+I), which extends perpendicularly to the helix axis and covers the N-terminal and C-terminal regions of actin. In the *presence* of Ca^{2+}, the C-terminal region of actin became more exposed, and troponin(C+I) became V-shaped with one arm extending towards the pointed end of the actin filament. This structure can be considered to show the location of troponin(C+I) in at least one of the states of skeletal muscle thin filaments. These Ca^{2+}-induced changes of troponin(C+I) provide a clue to the regulatory mechanism of contraction.

Key words: Ca^{2+}, electron cryomicroscopy, striated muscle, tropomyosin, troponin.

Troponin is a Ca^{2+}-binding protein present in vertebrate skeletal and cardiac muscle (striated muscle). Ca^{2+}-dependent regulation of striated muscle requires the regulatory proteins troponin and tropomyosin (*1*). When the concentration of Ca^{2+} is below micromolar, the interaction between actin and myosin is inhibited by troponin-tropomyosin. Binding of Ca^{2+} to troponin-C neutralizes the inhibition and the actin-myosin interaction is triggered. However, the molecular mechanism by which the Ca^{2+}-signal is transmitted from troponin(C+I) to other components of thin filaments, *i.e.*, troponin-T, tropomyosin, and actin, is unknown. The location of troponin on the thin filaments is also unknown, although the Ca^{2+}-induced dislocation of tropomyosin has been extensively studied. To elucidate the regulatory mechanism, it is important to determine the location of troponin on the surface of actin filaments in the presence and absence of Ca^{2+} as well as that of tropomyosin.

To explain the molecular mechanism of Ca^{2+} regulation, the steric blocking model was proposed on the basis of the change in X-ray diffraction (*2-4*). In this model, the location of tropomyosin is of primary importance. According to this model, tropomyosin molecules sterically block the myosin-binding site of actin in the absence of Ca^{2+}. To examine this model, the position of tropomyosin and its movement have been studied by three-dimensional electron microscopy (*5-13*) and X-ray diffraction (*14, 15*). It has been shown that tropomyosin is located on the surface of the outer domain [subdomain 1 and 2 (*16*)] without Ca^{2+} (*9-11*) and on the surface of the inner domain (subdomain 3 and 4) with Ca^{2+}. An azimuthal shift of tropomyosin position has been observed by electron microscopy (*9-11*). On the other hand, other studies using fluorescence resonance energy transfer spectroscopy (*17*), X-ray diffraction (*18*), and polarized fluorescence (*19*) failed to detect significant movement of tropomyosin. In addition, modeling studies pointed out that the Ca^{2+}-induced change of intensity in the X-ray diffraction patterns cannot be explained only by the movement of tropomyosin. The unidentified change of intensity was mainly explained by the structural change of actin (*20-22*), however the possibility of structural change of troponin has also been suggested (*23*). It is known that the tropomyosin position in the absence of Ca^{2+} is more difficult to determine with electron cryomicroscopy. In previous works using electron microscopy or X-ray diffraction, it was assumed that the density due to troponin would not contribute to the three-dimensional images reconstructed by imposing helical symmetry and that tropomyosin follows the actin symmetry. These assumptions are probably less valid in the structure

[1] This work was supported by the system of special postdoctoral researchers of RIKEN (to T.I.), a Grant-in-Aid for General Scientific Research and Specially Promoted Scientific Research from the Ministry of Education, Science, Sports and Culture of Japan, an HFSP grant and a grant for Biodesign Project of RIKEN (to T.W.).

[2] Present address: Laboratory of Structural Biology, NIAMS, National Institutes of Health Bethesda, MD 20892, USA.

[3] To whom correspondence should be addressed. Tel: +81-3-5802-4359, Fax: +81-3-5802-4359, E-mail: wakabayashi@phys.s.u-tokyo.ac.jp

without Ca^{2+} than that with Ca^{2+}.

Troponin is Ca^{2+}-receptive protein (*1, 24*). Therefore, Ca^{2+}-induced change in thin filaments takes place first in troponin. This change in troponin would trigger tropomyosin movement or conformational changes of actin.

The other model for Ca^{2+} regulation is a cooperative/allosteric model (*25-31*), which does not necessarily require tropomyosin dislocation. According to this model, the inhibition of contraction is suppressed by the binding of myosin to actin: the transition from the T-state to the R-state is triggered either by Ca^{2+} or myosin in a similar manner as hemoglobin (*32*). A study using ATPase activity (*30*) shows these two states, the on-state and the off-state, exist both in the presence and in the absence of Ca^{2+}. In the off-state, thin filaments do not allow actomyosin ATPase activation, but this does occur in the on-state. Further studies on ATPase activity (*31, 33*) showed that a three-state model is required. According to this model, open, closed, and blocked states coexist in the absence of Ca^{2+}, while open and closed states coexist in the presence of Ca^{2+}. In the open state, myosin and actin bind strongly and actomyosin ATPase is activated, whereas activation is not allowed in the closed and blocked states, in which binding is weak or absent, respectively. A model based on the cooperative/allosteric model that explains the result of fluorescence energy transfer (*34, 35*) and X-ray diffraction study (*18*) was proposed (*36*). In this model, the location of tropomyosin is not determined by Ca^{2+} concentration, whereas troponin-I movement is induced by Ca^{2+}. The result of site-directed mutagenesis introduced in the subdomain 4 of actin cannot be explained by the simple steric block model (*37*). A model that incorporates both a steric block model and a cooperative/allosteric model is required to explain the higher activation of myosin ATPase by the mutant actin in the presence of tropomyosin-troponin and Ca^{2+} in comparison with that without regulatory proteins (*37*). The states of the cooperative/allosteric model correspond to the change of conformation or location of tropomyosin, troponin, and/or actin. To clarify the molecular details of the allosteric mechanism, it is important to determine the structure of each component of thin filaments.

The three-dimensional structure of troponin-C in crystal or solution with or without Ca^{2+} has been determined (*38-41*). It is reported that the N-terminal fragment of troponin-I binds to troponin-C in the presence of Ca^{2+} (*42*). It is also known that the N-terminus and C-terminus of troponin-I play an important role in regulation (*43*). The C-terminal region of troponin-I moves away from the C-terminal region of actin (Cys374) and closer to Cys98 of troponin-C when Ca^{2+} ions bind to troponin-C (*44*). Thus, to elucidate the regulatory mechanism, it is important to reveal the Ca^{2+}-induced changes in the location and conformation of troponin in the thin filaments of striated muscle. Though the locations of other actin-binding proteins [calponin (*45*), caldesmon (*46*), scruin (*47*), α-actinin (*48*), and fimbrin (*49*)] have been reported, that of troponin in the thin filaments could not be determined. Because troponin binds to actin in the stoichiometric ratio of 1:7 (*50*), it does not follow the helical symmetry of actin and three-dimensional reconstruction using actin helical symmetry cannot reveal the location of troponin. This difficulty could be overcome by binding troponin(C+I) to actin in an almost stoichiometric ratio. This allowed us to impose helical symmetry to solve the three-dimensional structure including troponin(C+I).

Troponin(C+I) on the thin filaments *without* or *with* Ca^{2+} could be visualized in the three-dimensional images reconstructed from electron cryomicrographs to about 2.5 nm or 3 nm resolution, respectively. Images of 4,368 and 2,352 actin molecules at different levels of defocus were required to obtain the structure *without* or *with* Ca^{2+}, respectively. To allow detailed evaluation of the regions due to troponin(C+I) in the three-dimensional map *without* or *with* Ca^{2+}, the three-dimensional image of actin-tropomyosin without troponin(C+I) was also reconstructed to about 2.5 nm resolution by combining images of 4,032 actin molecules.

MATERIALS AND METHODS

Specimen Preparation—Skeletal muscle troponin and tropomyosin (*51*) and actin (*52*) were prepared from rabbit back muscle. Troponin(C+I) was separated from troponin by ion exchange chromatography (*51*). Thin filaments were reconstituted from actin, tropomyosin, and troponin(C+I). Tropomyosin and troponin(C+I) were mixed, and the mixture was centrifuged for 10 min at 360,000×g in a Beckman TL-100 ultracentrifuge to remove aggregates. G-actin was added to the supernatant, and the mixture was incubated for 10 min at 25°C. The final solution consisted of 2.3 μM actin, 0.38 μM tropomyosin, 23 μM troponin(C+I), 100 mM NaCl, 5 mM $MgCl_2$, 10 mM imidazole-HCl (pH 7.4), and 50 μM $CaCl_2$ or 2 mM EGTA.

Determination of Stoichiometry of Binding of Troponin-(C+I) to Actin—Reconstituted thin filaments were centrifuged, and the resultant pellet and supernatant were applied to SDS-PAGE (*53*). Following densitometry of the gel, the densities of actin, troponin-C, and troponin-I in the pellet were compared. To exclude the contribution of free protein in solution contained in pellet, the densities of bands from the supernatant was subtracted from those from the pellet. The amounts of protein in the bands were determined from a calibration curve, which was drawn by measuring the density of bands produced by applying various amounts of proteins to the gels. The protein concentration was determined using the absorption at 280 nm (*25*).

Electron Cryomicroscopy—A specimen of actin-tropomyosin-troponin(C+I) complex in the presence of free troponin(C+I) was mounted on holey carbon film and plunged into an ethane slush (*54*). Grids were examined with an electron microscope (HF2000, Hitachi) equipped with a cold field-emission gun at 200 kV. A Gatan cold stage was used. Micrographs were recorded at a nominal magnification of 30,000× on Kodak SO163 film. The electron dose was about 15 $e^-/Å^2$. To get good coverage of the defocus, images were collected at different levels of defocus between 2 and 4 μm (*11*).

Image Analysis—Individual images of filaments were digitized with a CCD film scanner (LeafScan45, Scitex) using a step size of 5 μm per pixel, corresponding to 0.17 nm on the specimen. The images of curved filaments were straightened (*55*) and helical reconstruction was carried out in the standard way (*56*) using the selection rule of $l=-13n+28m$ (true pitch=76.7 nm). The programs of

MRC (Cambridge) (*57*) were used with slight modification. Three helical repeats (6 crossovers) were boxed, interpolated and floated into an array of size 256×2,048, and Fourier-transformed, and 20 layer-lines were extracted. Near- and far-side data were averaged and the raw image phases were corrected for the contrast transfer function (CTF) determined by the degree of underfocus, which was estimated from the computed diffraction pattern of a carbon film near the filament images. Seven (in the *presence* of Ca^{2+}) or 13 (in the *absence* of Ca^{2+}) images of troponin(C+I)-containing filaments were averaged. The refinement of the underfocus was carried out iteratively using the phase residual between the averaged filament and individual filaments. The amplitudes and phases of the averaged filament were corrected for the averaged contrast transfer function (aCTF) of the images. As a control image, 12 images of actin-tropomyosin were averaged.

RESULTS AND DISCUSSION

Binding of Troponin(C+I) to Actin-Tropomyosin—Figure 1 shows that actin was almost fully saturated with troponin(C+I) (molar ratio of 1:0.7 instead of 7:1) when troponin(C+I) was added at a high concentration. In the presence of Ca^{2+}, a higher concentration [23 μM troponin-(C+I) to 2.3 μM actin] of troponin(C+I) was required for saturation. Troponin(C+I) now follows actin symmetry: the density due to troponin(C+I) can be visualized in the three-dimensional images obtained by helical reconstruction. A detailed evaluation of the density due to troponin-(C+I) was possible by comparing the structure of actin-tropomyosin-troponin(C+I) with that of actin-tropomyosin without troponin(C+I). Biochemical assay showed that the actin-activated myosin subfragment-1 (S1) ATPase was completely inhibited irrespective of Ca^{2+} concentration when troponin(C+I) bound to actin-tropomyosin in the molar ratio of 0.7:1. When a lower amount of troponin(C+I) was added to actin-tropomyosin, troponin-(C+I) bound to actin-tropomyosin in a Ca^{2+}-dependent manner (less binding in the *presence* of Ca^{2+}), indicating that most troponin(C+I) molecules bind to actin filaments through tropomyosin in the presence of Ca^{2+}, because the binding of troponin(C+I) to actin was found to require the presence of tropomyosin in the presence of Ca^{2+}. Moreover, actin-activated myosin subfragment-1 ATPase was regulated by Ca^{2+} concentration as reported previously (*58*).

Ca^{2+}-Induced Structural Change in Actin-Tropomyosin-Troponin(C+I) Filaments—Figure 2 shows general views of electron cryomicrographs of actin-tropomyosin-troponin(C+I) either *without* Ca^{2+} (Fig. 2a) or *with* Ca^{2+} (Fig. 2b). Figure 3 shows the computed diffraction pattern of the projection of the averaged three-dimensional image of actin-tropomyosin-troponin(C+I) either *without* Ca^{2+} (Fig. 3a) or *with* Ca^{2+} (Fig. 3b). Figure 4 shows the amplitude and phase angle distribution of the averaged data sets as solid lines and dotted lines, respectively. Ca^{2+}-induced change of the amplitude distribution can be observed in the fifth layer-line ($l=11$, $n=-3$) with spacing of 1/70 Å (Fig. 4c). This result is different from that of an X-ray diffraction study on frog muscle (*59*). Our specimens contain much higher amount of troponin(C+I) than frog muscle, and this may be the origin of apparent discrepancy. Figure 3c shows the corresponding diffraction pattern of actin-tropomyosin that was used as control data to evaluate the density due to troponin(C+I). The intensity of the actin-tropomyosin layer-line with 1/70 Å spacing was much weaker (Figs. 3c and 4c), indicating that the intensity of this layer-line reflects the Ca^{2+}-induced change of troponin(C+I). The maximum amplitude of the actin-tropomyosin-troponin(C+I) layer-line with 1/190 Å spacing was increased by 46% by Ca^{2+} binding compared to the layer-line with 1/380 Å spacing. This increase is much larger than that deserved by X-ray diffraction study: the X-ray diffraction intensity of the non-overlap muscle increased by 15% on activation (*20*). It has been assumed that the amplitude of the layer-line with 1/190 Å spacing is affected by both tropomyosin and actin. The changes in troponin-(C+I) may also contribute to this layer-line. This explains why the increase in the amplitude is larger in our specimens that contain much more troponin(C+I). The phase residual is 21.7° up to 2.5 nm resolution in the *absence* of Ca^{2+}, 43.7° up to 2.5 nm and 40.2° up to 3 nm in the *presence* of Ca^{2+}. The phase residual is better in the *absence* of Ca^{2+}. This might be due to tighter binding of troponin(C+I) to actin in the *absence* of Ca^{2+}.

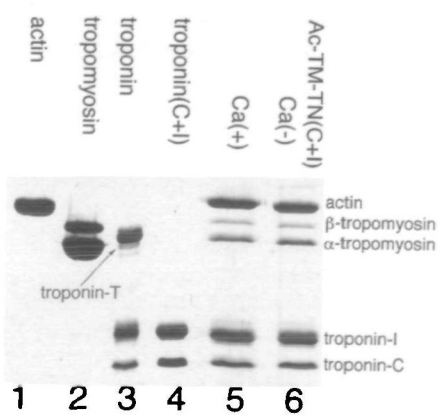

Fig. 1. **SDS-PAGE pattern of actin, tropomyosin, troponin(C+I), and reconstituted thin filaments.** Lanes: 1, actin; 2, tropomyosin; 3, troponin(C+I+T); 4, troponin(C+I); 5, actin-tropomyosin-troponin(C+I) in the *presence* of Ca^{2+}; 6, in the *absence* of Ca^{2+}. Troponin(C+I) molecules bind to actin molecule in an almost stoichiometric ratio (0.7:1) according to the calibrated densitometry of the gel.

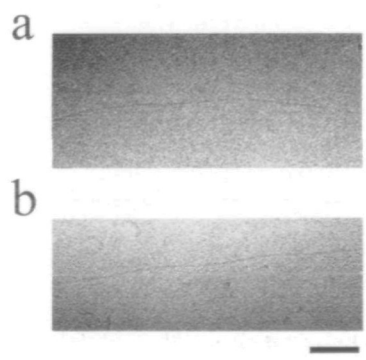

Fig. 2. **Overviews of electron cryomicrographs of thin filaments reconstituted from actin, tropomyosin, and troponin(C+I).** (a) *Without* Ca^{2+}, (b) *with* Ca^{2+}. (Proteins were purified from rabbit skeletal muscle.) Protein is black. Scale bar, 100 nm.

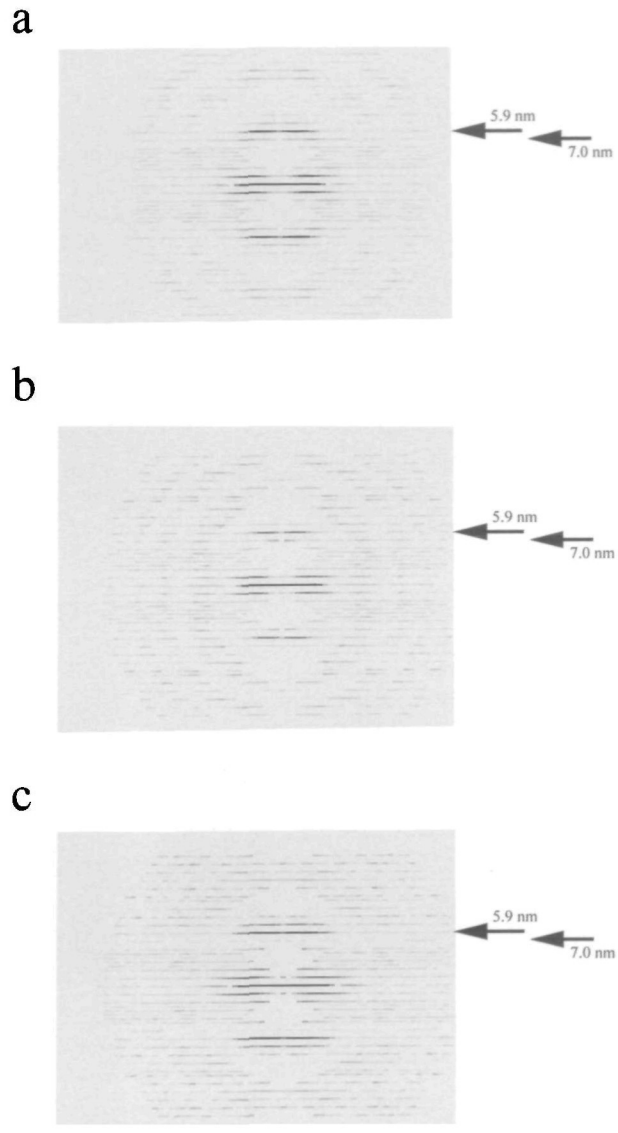

Fig. 3. Computed diffraction patterns of filaments with the length of 12 crossovers reconstituted from actin, tropomyosin, and troponin(C+I) in the *absence* (a) and in the *presence* (b) of Ca^{2+} after averaging and the correction of contrast transfer function. The regions with low amplitude are mainly due to the structure factor (not the contrast transfer function).

The three-dimensional structure of thin filaments reconstituted from the electron cryomicrographs of actin-tropomyosin-troponin(C+I) is shown in Fig. 5(a, b) together with that of actin-tropomyosin without troponin(C+I) (Fig. 5c). The three-dimensional images were reconstructed by imposing the helical symmetry of actin. To compare them with the atomic model of actin filaments (*60*), they were fitted to the atomic model. The reconstructed images superimposed on the atomic model are shown in Figs. 6 and 7. Detailed comparison of the density maps is possible using the atomic model as a reference structure. A dramatic Ca^{2+}-induced change can be observed by comparison of the map in the *absence* of Ca^{2+} (Figs. 5a, 6a and 7a) with that in the *presence* of Ca^{2+} (Figs. 5b, 6b, and 7b).

Location and Conformation of Troponin(C+I)—To examine the location of troponin(C+I), we compared the three-dimensional structure of actin-tropomyosin-troponin(C+I) with that of actin-tropomyosin. Extra regions were observed only in the former. In the *absence* of Ca^{2+} (Fig. 6a), the density near the subdomain 1 of actin (indicated by arrows) is higher than that in the actin-tropomyosin (Fig. 6c). This high-density region extends horizontally (perpendicularly to the helix axis) from the N-terminal region of actin and covers the C-terminal region of actin. In the *presence* of Ca^{2+} (Fig. 6b), the extra density protrudes almost vertically (parallel to the helix axis) from the N-terminus of actin in the direction of the pointed end of actin (indicated by arrows in Fig. 6b). These regions of high density are absent in actin-tropomyosin (Fig. 6c). The extra density in the *presence* of Ca^{2+} is 40 Å in height along the actin helix axis and 20 Å in thickness in the radial direction, and the density appears outside of the subdomain 1 of the atomic model of actin in the *absence* of Ca^{2+}. Thus, we interpreted these extra-density regions indicated by arrows being *mainly* due to troponin(C+I). It is possible that these regions partly include actin. To evaluate the contribution from troponin(C+I) and actin, the volume of these regions was measured. It was 18 or 26% of the expected volume calculated from the molecular weight of troponin(C+I) in the *absence* of Ca^{2+} or in the *presence* of Ca^{2+}, respectively. Though the measured volumes of the extra-density regions in both cases are smaller than the expected value, it is still too large to be explained only by the conformational change of actin, as described in the next section. The smaller value may be due to the fluctuation of troponin(C+I), which results in the decrease of density when three-dimensional reconstruction was done by imposing helical symmetry.

Structural Change of Actin—Figure 7a shows that some α-carbon atoms of actin lie outside of the red contour line based on electron cryomicrographs of actin-tropomyosin-troponin(C+I) in the *absence* of Ca^{2+}, whereas almost all α-carbon atoms are inside the line in the *presence* of Ca^{2+} (Figs. 6b and 7b). The α-carbon atoms outside of the contour line are in residues 222-233 of the subdomain 4 of actin. Without troponin(C+I), the region around residues 222-233 shows similar features to that of actin-tropomyosin-troponin(C+I) in the *presence* of Ca^{2+}. This suggests that the distance between the inner domain (subdomain 3 and 4) and the outer domain (subdomain 1 and 2) is slightly smaller in the *absence* of Ca^{2+}. This result is consistent with the result of the modeling based on X-ray diffraction (*21, 22*), which proposes an increase in the distance between the inner domain and the outer domain in the presence of Ca^{2+}. It should be pointed out that the mass representing the α-carbon atoms outside of the red contour in Fig. 7a is much smaller than the extra mass we described in the previous section. This is why we assigned the extra mass *mainly* to troponin(C+I), even though a minor contribution from actin cannot be excluded.

Assignment of Tropomyosin—The three-dimensional map of actin-tropomyosin fits well to the atomic model except for the regions that cannot be assigned to actin (indicated by an arrowhead in Fig. 6c or enclosed by a dotted circle in Fig. 7c). These regions lie on the outer surface of the inner domain of actin [the subdomain 3 and the subdomain 4 (*14*)]. The radius from a helix axis is 3.8 nm. We assigned this region to tropomyosin, because it extends along the long-pitched helix. It has been difficult to

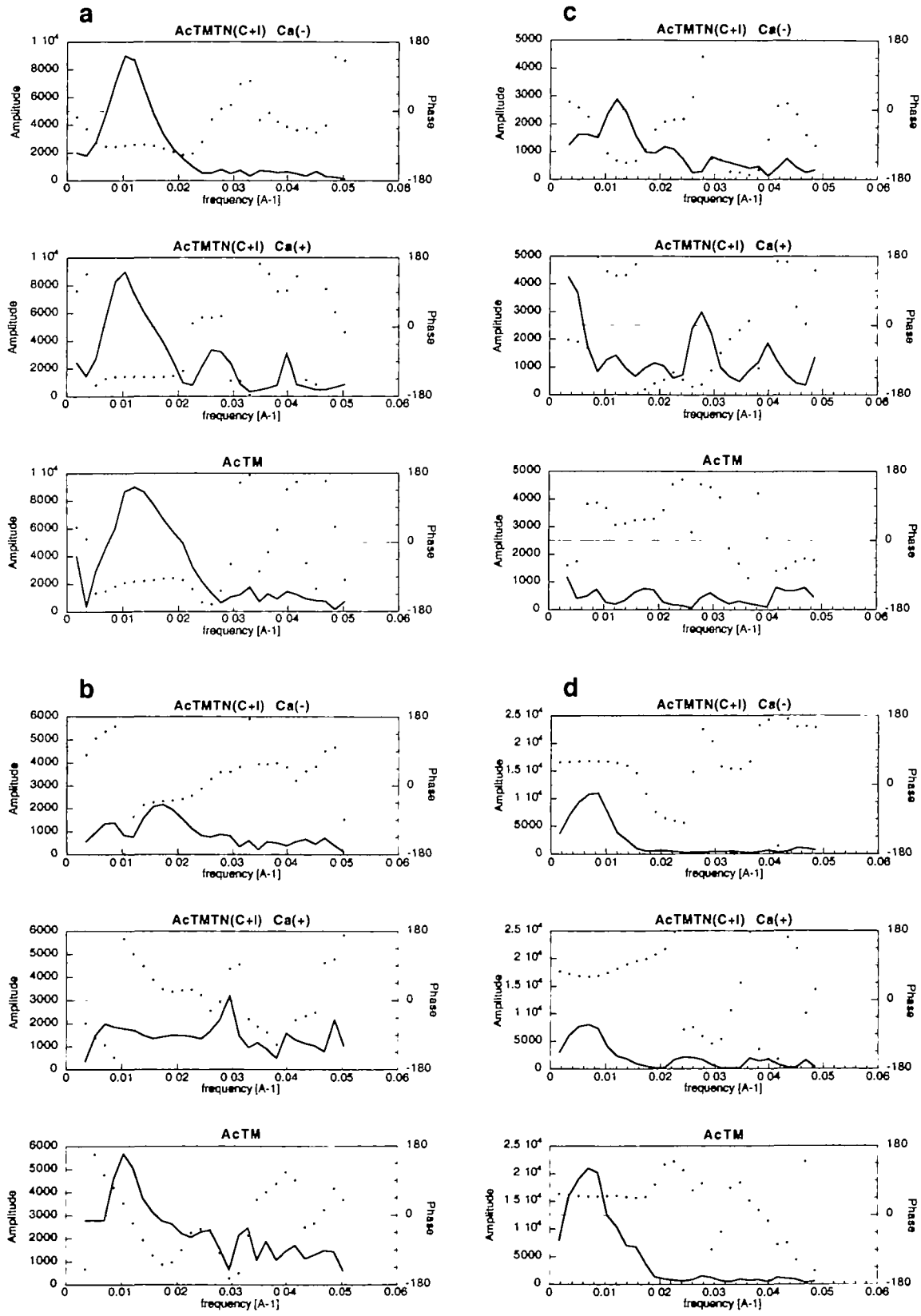

Fig. 4. Amplitude (solid lines) and phase angles (dotted lines) of computed diffraction patterns of averaged filaments. (a) First layer-line ($n=2$, $l=2$), (b) second layer-line ($n=4$, $l=4$), (c) fifth layer-line ($n=-3$, $l=11$), and (d) sixth layer-line ($n=-1$, $l=13$). Ca^{2+}-induced changes in the amplitude distribution of the fifth layer-line ($n=-3$, $l=11$) with the spacing of 1/70 Å can be observed. Ca^{2+}-induced increase in the amplitude of the second layer-line is observed in comparison with that of the first layer-line.

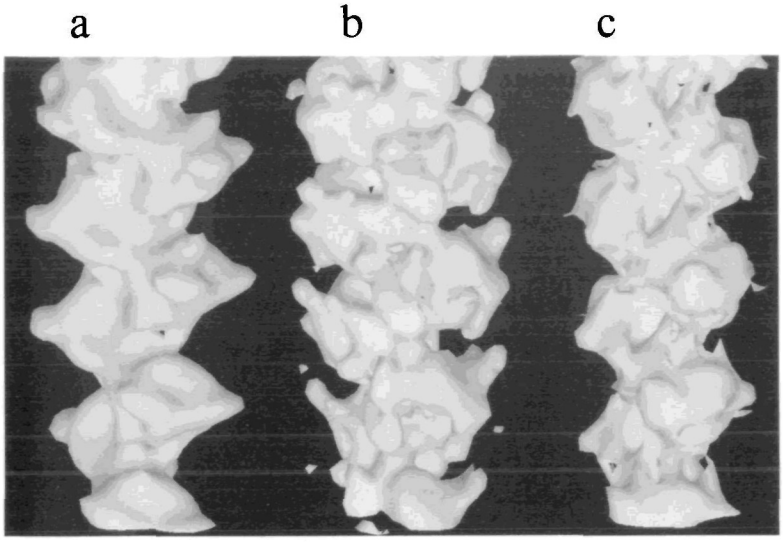

Fig. 5. **Oblique views of three-dimensional structure of thin filaments reconstructed from electron cryomicrographs.** (a) Actin-tropomyosin-troponin-(C+I) in the *absence* of Ca^{2+}, (b) in the *presence* of Ca^{2+}, (c) actin-tropomyosin. Density cut-off level was chosen so that 100% of the expected volume is recovered. Below: barbed end (towards Z-line), above: pointed end (towards M-line). AVS system is used for visualization (*66*).

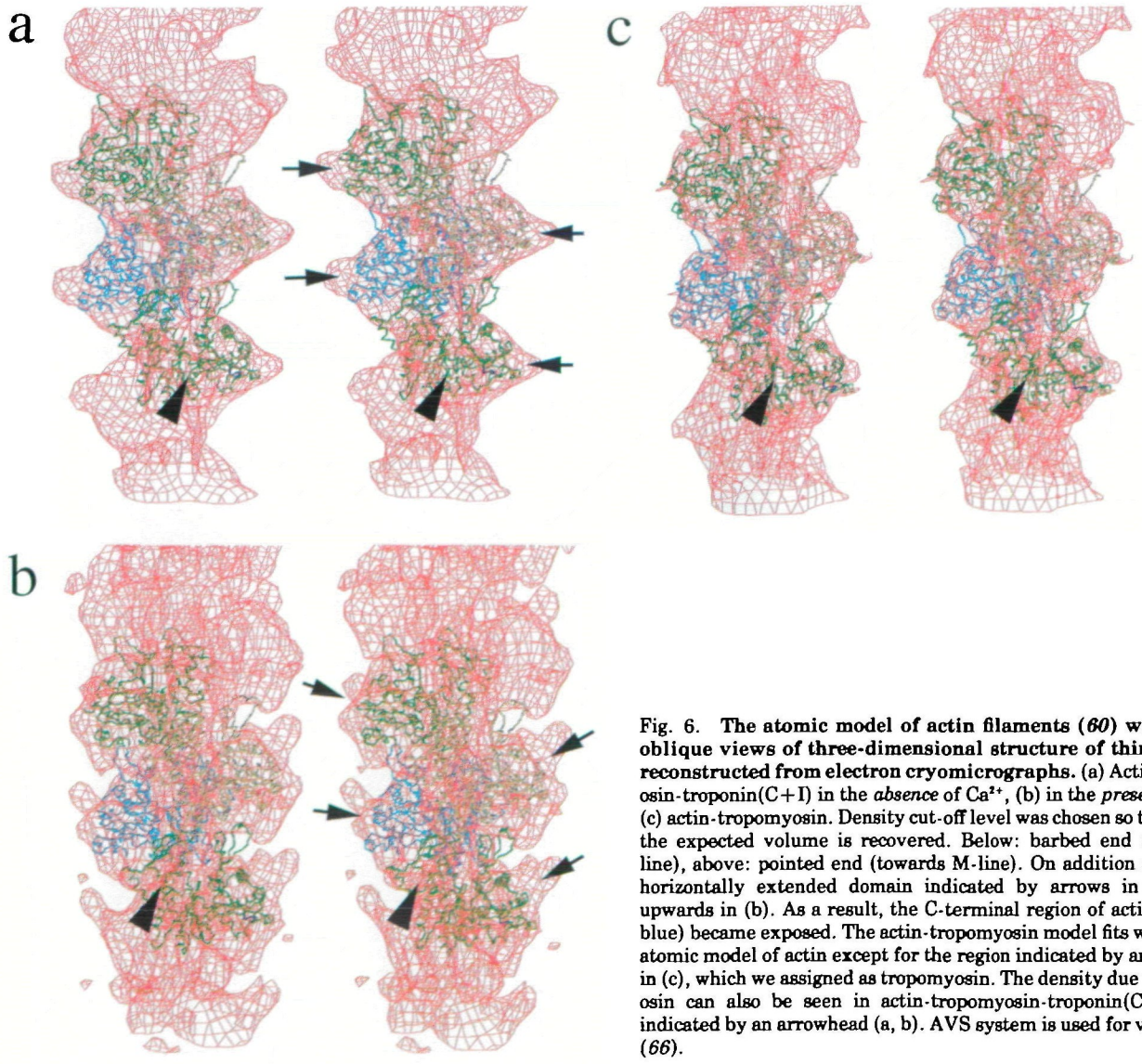

Fig. 6. **The atomic model of actin filaments (*60*) was fitted to oblique views of three-dimensional structure of thin filaments reconstructed from electron cryomicrographs.** (a) Actin-tropomyosin-troponin(C+I) in the *absence* of Ca^{2+}, (b) in the *presence* of Ca^{2+}, (c) actin-tropomyosin. Density cut-off level was chosen so that 100% of the expected volume is recovered. Below: barbed end (towards Z-line), above: pointed end (towards M-line). On addition of Ca^{2+}, the horizontally extended domain indicated by arrows in (a) moved upwards in (b). As a result, the C-terminal region of actin (shown in blue) became exposed. The actin-tropomyosin model fits well with the atomic model of actin except for the region indicated by an arrowhead in (c), which we assigned as tropomyosin. The density due to tropomyosin can also be seen in actin-tropomyosin-troponin(C+I) and is indicated by an arrowhead (a, b). AVS system is used for visualization (*66*).

visualize tropomyosin as continuous strands in unstained states at neutral pH. Previously, unstained tropomyosin could be visualized as continuous strands only after decoration with myosin subfragment-1 (*7, 8*), which seems to stabilize tropomyosin. Our present result shows unstained tropomyosin in the absence of the myosin moiety for the first time. It is also consistent with our previous results (*11, 12*).

A similar feature can be observed in the actin-tropomyosin-troponin(C+I) maps. This is also interpreted as tropomyosin and enclosed by a dotted circle in Fig. 7, a and b. Tropomysin seems to move by 20° (1.5 nm) towards the inner domain in the *presence* of Ca^{2+}. The similar density in actin-tropomyosin exists in the almost same location as that of actin-tropomyosin-troponin(C+I) in the *absence* of Ca^{2+} (Fig. 7c). This is consistent with the three-state model (*33*) in which tropomyosin in actin-tropomyosin is mainly in the closed state in the absence of the myosin moiety. The position of tropomyosin in the *presence* of Ca^{2+} is consistent with the result of site-directed mutagenesis (*37*): after mutagenesis in subdomain 4, the mutant actin bound tropomyosin poorly. However, the extent of movement of tropomyosin is smaller than that expected from the steric blocking model (*2-5*). It is probable that troponin-T, which is absent in our specimens, is required to tightly link the Ca^{2+}-induced changes in troponin(C+I) with the movement of tropomyosin. If troponin-T plays the role of linking tropomyosin with troponin(C+I), it is possible that tropomyosin moves further (*2-5, 10*) in the presence of troponin-T. As mentioned above, it was found that the binding of troponin(C+I) to actin requires tropomyosin. Thus, tropomyosin is considered to play an important role in the binding of troponin(C+I) to the actin filament. However, in the three-dimensional map, troponin(C+I) does not appear to make direct contact with tropomyosin. Therefore, it is possible that tropomyosin causes a conformational change of actin and facilitates the binding of troponin(C+I) to the actin filament.

It is interesting that the hydrophobic α-helix of actin corresponding to residues 338-348 (shown in Fig. 6 in blue, in Fig. 7 in dark blue), which is considered to interact with myosin (*61*), is exposed in the *presence* of Ca^{2+} but covered by tropomyosin in its *absence*. This supports the steric block model. In the presence of troponin-T, troponin(C+I) binds to actin in the molar ratio of 1:7. In this case, both the N-terminal and C-terminal regions of at least six of the seven actin molecules are exposed, if tropomyosin does not cover them. We propose that myosin can be activated by actin only when the N-terminal and C-terminal regions and the hydrophobic α-helix (residues 338-348) of actin are exposed. Troponin-T was removed in our specimens, and the N-terminal regions of all actin monomers are covered by troponin(C+I) even in the *presence* of Ca^{2+}. Thus, actin-activated ATPase of S1 is inhibited even in the *presence* of Ca^{2+}, when troponin(C+I) binds to actin in the molar ratio of 1:1. In a cooperative/allosteric model, thin filaments are present as a mixture of the on-state (open state) and off-state (closed or blocked state) irrespective of Ca^{2+} concentration. The C-terminus of actin is covered by troponin(C+I) in actin-tropomyosin-troponin(C+I) filaments *without* Ca^{2+}. This may represent the off-state (probably blocked state) of thin filaments.

Significance of Structural Difference—To show the statistical significance of the difference in density *mainly* due to troponin(C+I), *t*-maps and the variance maps were examined. Figure 8 shows the resultant images of Student's *t*-test (*7*), which reveals that the density of the regions indicated by arrows in Fig. 6, a and b, is significantly higher (*with* Ca^{2+}, $t>2.7$, corresponding to 98.5% confidence; and *without* Ca^{2+}, $t>2.2$, corresponding to 96% confidence) than that of actin-tropomyosin. These regions in red are superimposed on the three-dimensional image of actin-tropomyosin (Fig. 8). These red regions cover the N-terminus of actin and extend towards the C-terminus of actin in the *absence* of Ca^{2+} but towards the pointed end, so that the C-terminus becomes exposed, in the *presence* of Ca^{2+}. The interpretation we gave above (Figs. 6a, 6b, 7a, and b) is confirmed by Student's *t*-test. In these red regions, the

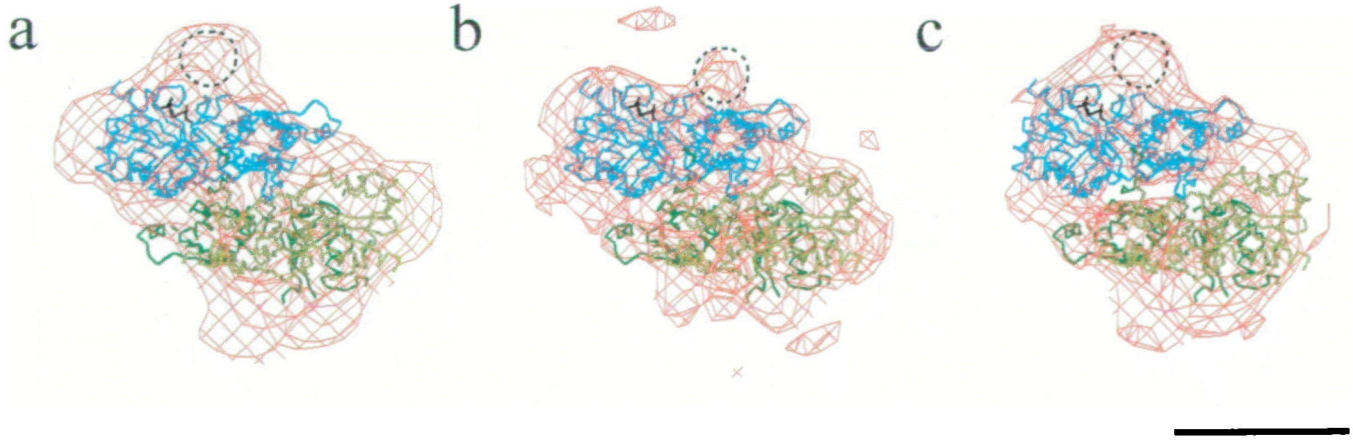

Fig. 7. **Top views (from pointed end) of the three-dimensional structure of thin filaments reconstructed from electron cryomicrographs fitted to the atomic model of actin filaments (*60*).** (a) Actin-tropomyosin-troponin(C+I) in the *absence* of Ca^{2+}, (b) in the *presence* of Ca^{2+}, (c) actin-tropomyosin. In the *presence* of Ca^{2+}, the C-terminal region of actin (shown in dark blue) became exposed. The actin-tropomyosin model fits well with the atomic model of actin except for the region indicated by a dotted circle in (c), which we assigned as tropomyosin. The density due to tropomyosin can also be seen in actin-tropomyosin-troponin(C+I) and is encircled (a, b). AVS system is used for visualization (*66*). Scale bar, 5 nm.

density of actin-tropomyosin-troponin(C+I) is significantly higher than that of actin-tropomyosin. The difference in densities between actin-tropomyosin-troponin(C+I) and actin-tropomyosin is high, and the variance of the density of actin-tropomyosin-troponin(C+I) should be low in these regions. Therefore, we interpret these regions as the part of troponin(C+I) that binds tightly to actin-tropomyosin.

To visualize the part of troponin(C+I) that binds less stably, we prepared variance maps (Fig. 9). The variance of the density in the mixture of three-dimensional density maps of actin-tropomyosin *and* actin-tropomyosin-troponin(C+I) was calculated to examine the regions where two kinds of map differ. In the regions where the density of actin-tropomyosin and actin-tropomyosin-troponin(C+I) differs, the density should show large variance. These regions are shown in red on the surface of the solid models of actin-tropomyosin-troponin(C+I) in Fig. 9. There are three possible situations in which large variance would be observed: when the difference in density of actin-tropomyosin-troponin(C+I) and actin-tropomyosin is large; when the variance of the density of actin-tropomyosin-troponin(C+I) itself is large; and the variance of the density of actin-tropomyosin is large. In the first or second case, we can interpret these regions with high variance as being *mainly* due to troponin(C+I). The third case is not likely, because the regions with high variance are located outside of (i) actin-tropomyosin and (ii) the atomic model of the actin filament. Thus, we conclude that most of the regions with high variance represent troponin(C+I).

Troponin(C+I) Movement—Figure 10 shows a schematic diagram of the structural change of actin-tropomyosin-troponin(C+I) filaments. In the *absence* of Ca^{2+} (panel a in Figs. 4–10 and Fig. 10c), the region with high density, which we interpret as troponin(C+I), surrounds subdomain 1 of actin (*U*, *V*, and *T* in Fig. 10, a and c) and subdomain 2 (*U* in Fig. 10, a and c). It should be noted that the region *U* covers the part of both subdomain 1 and subdomain 2. It is located 3.8 nm from the helical axis and has a width of 5 nm (in the azimuthal direction), a thickness of 3 nm (in the radial direction), and a height of 5 nm (along the helical axis). According to Student's *t*-test (Fig. 8a), troponin(C+I) binds to actin, covers the region stretching from the N-terminus of actin over the C-terminus of actin, and extends towards subdomain 4 of an adjacent actin protomer (regions *T* and *V* in Fig. 10, a and c). The importance of the C-terminus of actin for the regulation was demonstrated by a deletion experiment: when three residues were deleted from the C-terminus of actin, the extent of inhibition of actomyosin ATPase by troponin-I decreased (*62*). This is consistent with our results, which show that the C-terminal region of actin is surrounded by troponin(C+I) much more closely in the *absence* of Ca^{2+} than its *presence*. Thus, the three residues (Lys, Cys, and Phe) of the C-terminal region of actin may be important for the binding of troponin(C+I) without Ca^{2+}.

In the *presence* of Ca^{2+} (the panel b in Figs. 5–10 and Fig. 10d), the extra high-density region *mainly* corresponding to troponin(C+I) is V-shaped (4 nm width, 2 nm thickness, and 4 nm height) and locates at 3.6 nm from the helix axis. We interpret this structure as that of troponin(C+I) in one of the states in the presence of Ca^{2+}. Thus, we conclude that troponin(C+I) changes its structure when the concentration of Ca^{2+} increases. This is consistent with the result of fluorescence resonance energy transfer spectroscopy, which showed that the distance between Cys133 and Cys48 of troponin-I is 1.5 nm longer with Ca^{2+} than without Ca^{2+} (*63*). The N-terminal region of actin is covered by troponin-(C+I) irrespective of the Ca^{2+} concentration: the region *V* (Fig. 10, a and c) *without* Ca^{2+} and the region *Y* (Fig. 10, b and d) *with* Ca^{2+} cover the N-terminal region of actin. It was

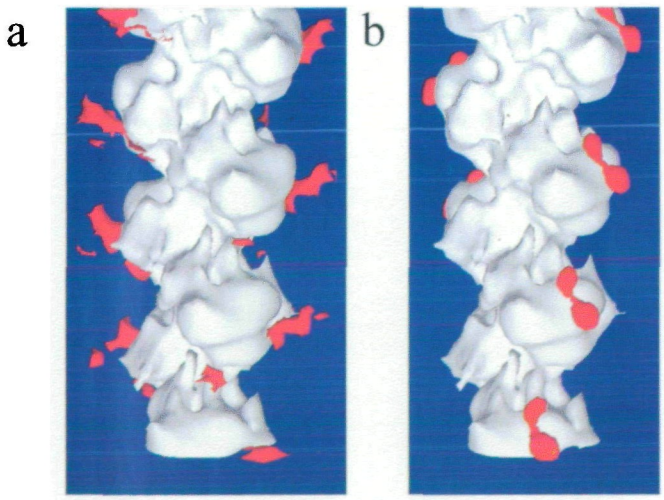

Fig. 8. **Student's *t*-map.** The regions where the density of actin-tropomyosin-troponin(C+I) in the *absence* or *presence* of Ca^{2+} is significantly higher than that of actin-tropomyosin are interpreted as the part of troponin(C+I) that binds to actin in a stable manner. These regions are shown in red by superimposing them on the solid model of actin-tropomyosin. In the *absence* of Ca^{2+}, troponin(C+I) binds tightly to actin around the C-terminal region of actin (a). In the *presence* of Ca^{2+} (b), however, troponin(C+I) binds tightly at the frontal part of the outer domain (subdomain 1+2) of actin. AVS system is used for visualization (*66*).

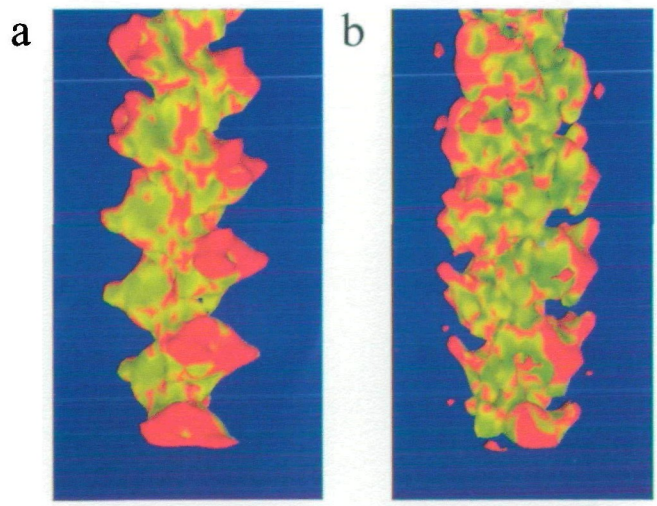

Fig. 9. **Variance maps.** The variance of the density of actin-tropomyosin and actin-tropomyosin-troponin(C+I) data sets is large in the regions shown in red on the solid models of actin-tropomyosin-troponin(C+I). These regions show the difference between the density of actin-tropomyosin-troponin(C+I) and actin-tropomyosin *without* (a) or *with* (b) Ca^{2+} and are interpreted as troponin(C+I) (that binds less firmly to actin) or tropomyosin that shifted. AVS system is used for visualization (*66*).

shown that the residues 96-115 of troponin-I bind to actin in the absence of Ca^{2+} but bind to troponin-C in the presence of Ca^{2+} (*64*). Thus, the region *T* shown in Fig. 10, a and c, may correspond to the inhibitory peptide (residues 96-115) of troponin-I: this region *T* binds to the N-terminal region of actin only in the *absence* of Ca^{2+}. The *X* region (Fig. 10, b and d) protrudes almost along the helical axis. This kind of structural change cannot be explained by movements of troponin(C+I) as a rigid body: conformational changes of troponin(C+I) itself must have occurred. This is consistent with the small-angle scattering experiments (*65*). It will be interesting to fit the atomic model to the reconstructed thin filament images when the crystal structure of troponin(C+I) becomes available. This will allow the large changes in the three-dimensional structure of the actin-tropomyosin-troponin(C+I) to be evaluated at an atomic level.

Comparison with Allosteric/Cooperative Model or Three-State Model—Figure 11 shows a schematic representation of the structural change of thin filaments based on our results of electron cryomicroscopy of actin-tropomyosin-troponin(C+I) *without* or *with* Ca^{2+}. To focus on the Ca^{2+}-induced changes in the interaction of troponin(C+I) with actin, the shift of tropomyosin and the Ca^{2+}-induced conformational changes of troponin(C+I) revealed in this work are *not* illustrated. In the *absence* of Ca^{2+}, troponin-(C+I) binds tightly to the N- and C-terminal regions of actin (Fig. 11, bottom left) and actin can not activate S1-ATPase. When Ca^{2+} binds to troponin-C, the binding of troponin(C+I) to actin becomes weaker and the C-terminus region of actin is exposed. However, in the absence of troponin-T (as in our specimens) the binding of troponin-(C+I) to the N-terminus region of actin was observed (Fig. 11, middle and bottom right). It is expected that the binding to the N-terminus of actin becomes much weaker (Fig. 11, middle and top right) in the presence of troponin-T. The "open state" in a three-state model is illustrated in the top right panel.

Comparison with Other Structural Studies—Our result shows that troponin(C+I) binds to both the N- and C-termini of actin in actin-tropomyosin-troponin(C+I) filaments in the *absence* of Ca^{2+} and to the N-terminus alone in the *presence* of Ca^{2+}. Structural studies using three-dimensional electron microscopy have identified the N-terminus of actin as a likely binding site for caldesmon (*46*), and the C-terminus of actin as a binding site for caldesmon (*46*), fimbrin (*49*), calponin (*45*), and α-actinin (*48*). These results demonstrate the N- and C-terminal regions of actin are important for its interaction with other proteins. Though troponin(C+I) extends to subdomain 2 in the same actin molecule in the *presence* of Ca^{2+}, it extends perpendicularly to the helical axis towards the adjacent actin protomer, which is located 27.5 Å away in the direction of the barbed end in the *absence* of Ca^{2+}. However, the tight binding of two consecutive actin protomers could not be observed. Actin-binding proteins such as caldesmon (*46*),

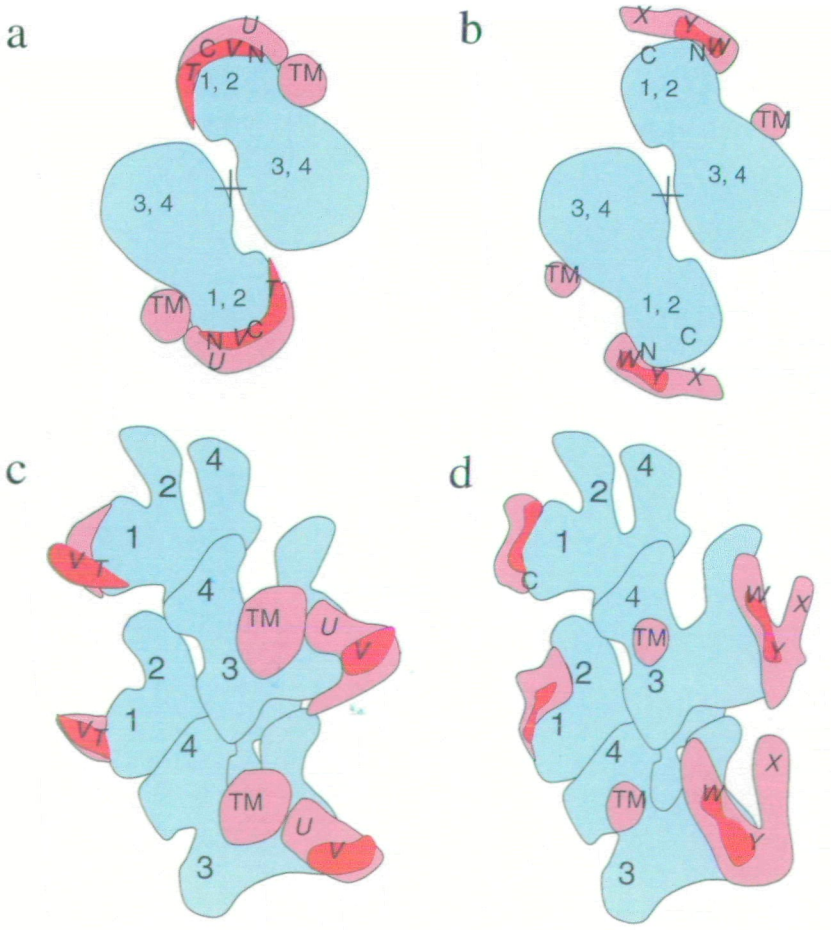

Fig. 10. Schematic representation of the binding of troponin(C+I) molecules to actin filaments in the *absence* (a, c) and in the *presence* of Ca^{2+} (b, d). (a) and (b) Top views, (c) and (d) side views. Actin and troponin(C+I) domains and tropomyosin density observed in Figs. 2 and 3 are labeled. 1, 2, 3, 4: subdomains of actin (*16*). N,C: N-terminus and C-terminus of actin. TM: tropomyosin. *T, U, V*: domains of troponin(C+I) *without* Ca^{2+}. *W, X, Y*: domains of troponin(C+I) *with* Ca^{2+}. The regions where the variance of the density is high (Fig. 9) were interpreted as troponin(C+I) or tropomyosin that shifted and are shown in pink. The regions where the value of Student's *t*-test is high (Fig. 8) were interpreted as the part of troponin(C+I) that binds to actin in a stable manner (*V, T without* Ca^{2+}; *W, Y with* Ca^{2+}). These regions are shown in red. Troponin(C+I) molecules are near the C-terminus of actin molecules in the *absence* of Ca^{2+}. *With* Ca^{2+}, however, troponin(C+I) covers mainly the N-terminus of actin and the C-terminal region of actin becomes exposed. We propose that the exposed C-terminus of actin may be an important prerequisite for activation of myosin ATPase and that the N-terminal region of actin and the hydrophobic α-helix corresponding to the residues 338-348 must be also exposed for actin-activation of myosin ATPase.

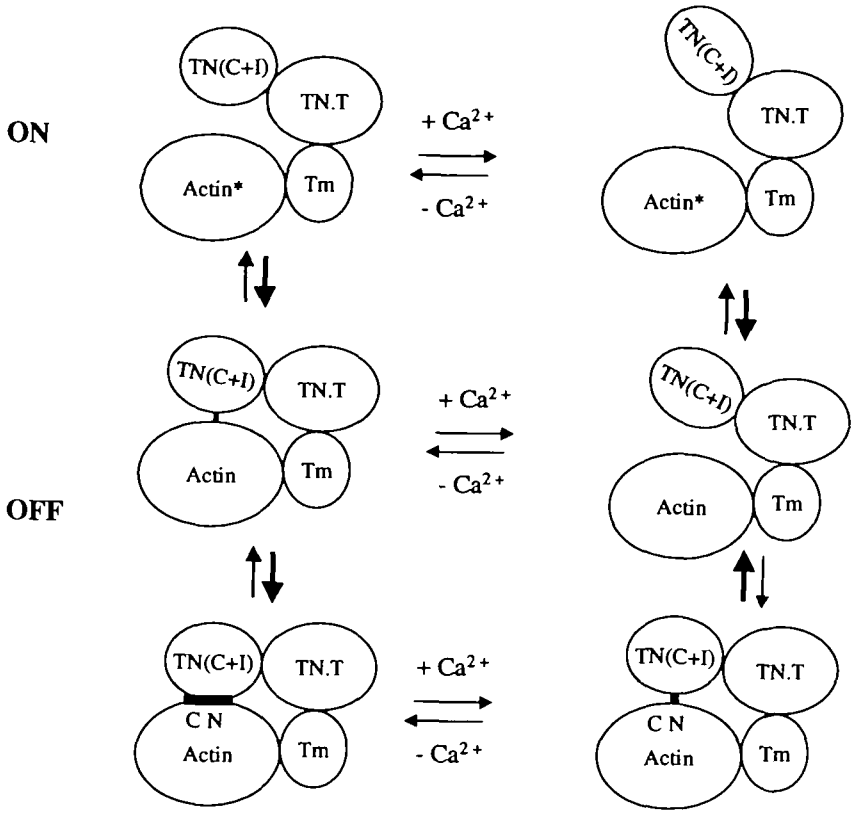

Fig. 11. **Schematic representation of the binding of troponin(C+I) with other components of thin filaments.** In the *absence* of Ca^{2+} (left column), troponin(C+I) binds to actin tightly (bottom left) at the N- and C-terminal regions. When Ca^{2+} binds to troponin-C (right column), binding of troponin(C+I) to actin becomes much weaker, and no binding to the C-terminal region of actin was observed (bottom right). According to the allosteric/cooperative model of Ca^{2+} regulation, thin filaments mainly assume a T-state (off-state, *i.e.*, closed or blocked state) that can not activate myosin ATPase. Myosin binding to actin converts actin in a T-state to an R-state (on-state, *i.e.*, open state) (actins marked with asterisks in a top row). Troponin(C+I) does not bind directly to actin in an R-state, and myosin ATPase is fully activated by actin (top right). As a result of the change in troponin-(C+I) binding to actin, tropomyosin shifts its position as shown in Fig. 7. This tropomyosin shift and conformational changes of troponin-(C+I) are omitted from the figure for simplicity.

fimbrin (*49*), calponin (*45*), α-actinin (*48*), and scruin (*47*) bind to two actin protomers along the long-pitched helix. Thus, troponin(C+I) binds to actin in a different way from these proteins. This is consistent with biochemical studies on caldesmon and calponin (*45, 46*).

The position of Cys133 of troponin-I can be estimated by comparing our result with that obtained by fluorescence resonance energy transfer spectroscopy or photo cross-linking (*17, 34*). The distance between Cys133 of troponin-I and the nucleotide is 3.3 nm in the absence of Ca^{2+} (*17*). The N-terminus of actin is 3.5 nm from the nucleotide (*16*). The region *V* cannot be a candidate for the location of Cys133 of troponin-I because it is located farther from the nucleotide than the N-terminus of actin. Cys133 should not be on the back side (C-terminal region) of actin, because the distance between Cys133 of troponin-I and Cys374 of actin is too long, *i.e.*, 4.2 nm in the absence of Ca^{2+} (*34*). This means that the region *T* also cannot be a candidate for the location of Cys133, because the distance between Cys374 of actin and the region *T* is much shorter than 4.2 nm. Therefore, it can be concluded that Cys133 of troponin-I should be located within or near the *U* region on the front side of actin in the *absence* of Ca^{2+}.

CONCLUSION

The three-dimensional image of actin-tropomyosin-troponin(C+I) showed remarkable Ca^{2+}-induced structural changes. The location of troponin(C+I) was examined by comparing the structure of actin-tropomyosin-troponin-(C+I) with that of actin-tropomyosin. The position of tropomyosin could be determined by fitting the atomic model of actin. Troponin(C+I) binds to the outer domain of actin and shows the Ca^{2+}-induced changes in its location and conformation. In the *absence* of Ca^{2+}, troponin(C+I) covers both N- and C-terminal regions of actin. These covered regions may represent the weak binding site of myosin on actin. It extends from the N-terminus of actin towards the C-terminus and the adjacent actin molecule. This structure may represent the blocked state, in which myosin cannot bind to actin. In the *presence* of Ca^{2+}, the C-terminal region of actin is exposed and troponin(C+I) becomes V-shaped. This clearly shows the Ca^{2+}-induced conformational change of troponin(C+I). This structure may represent one of the states assumed by thin filaments. In this structure, troponin(C+I) is still bound to the N-terminus of actin, and thin filaments can not activate myosin ATPase. We propose that the transition to the open state requires that both N- and C-terminal regions of the majority of actin protomers should *not* be covered by troponin(C+I). Troponin-T is expected to weaken the binding between actin and troponin(C+I) and facilitate the transition to the open state. The Ca^{2+}-induced detachment of troponin(C+I) from the C-terminal region of actin is reinforced by troponin-T, which facilitates the detachment of troponin(C+I) from the N-terminus of actin, leading ultimately to the open state of thin filaments and active interaction between actin and myosin.

We would like to thank Prof. Y. Inoue for making it possible for us to collaborate in this work. We also thank Dr. K. Nakazato and the computer centre of RIKEN for making the AVS system available. We are indebted to Dr. R.A. Crowther (MRC, Cambridge) for his kind suggestions about variance maps. Dr. Y. Meng kindly provided us the

programs to fit atomic model objectively. We would like to thank Mr. T. Yasunaga and Mr. Y. Matsuura for reading the manuscript and making kind suggestions. Dr. M. Kikkawa made many suggestion about graphics. We thank Drs Murray Stewart (MRC, Cambridge) and Alasdair C. Steven (NIH) for reading the manuscript.

REFERENCES

1. Ebashi, S. and Endo, M. (1968) Calcium ion and muscle contraction. *Prog. Biophys. Mol. Biol.* **18**, 123-183
2. Haselgrove, J.C. (1972) X-ray evidence for a conformational change in the actin-containing filaments of vertebrate striated muscle. *Cold Spring Harbor Symp. Quant. Biol.* **37**, 341-352
3. Huxley, H.E. (1972) Structural changes in the actin- and myosin-containing filaments during contraction. *Cold Spring Harbor Symp. Quant. Biol.* **37**, 361-376
4. Parry, D.A.D. and Squire, J.M. (1973) Structural role of tropomyosin in muscle regulation: analysis of the X-ray diffraction patterns from relaxed and contracting muscles. *J. Mol. Biol.* **75**, 33-55
5. Wakabayashi, T., Huxley, H.E., Amos, L.A., and Klug, A. (1975) Three-dimensional image reconstruction of actin-tropomyosin complex and actin-tropomyosin-troponinT-troponinI complex. *J. Mol. Biol.* **93**, 477-497
6. Toyoshima, C. and Wakabayashi, T. (1985) Three-dimensional image analysis of the complex of thin filaments and myosin molecules from skeletal muscle. IV. Reconstruction from minimal- and high-dose images of the actin-tropomyosin-myosin subfragment-1 complex. *J. Biochem.* **97**, 219-243
7. Milligan, R.A. and Flicker, P.F. (1987) Structural relationships of actin, myosin, and tropomyosin revealed by cryo-electron microscopy. *J. Cell Biol.* **105**, 29-39
8. Milligan, R.A., Whittaker, M., and Safer, D. (1990) Molecular structure of F-actin and location of surface binding sites. *Nature* **348**, 217-221
9. Lehman, W., Craig, R., and Vibert, P. (1994) Ca^{2+}-induced tropomyosin movement in *Limunus* thin filaments revealed by three-dimensional reconstruction. *Nature* **368**, 65-67
10. Vibert, P., Craig, R., and Lehman, W. (1997) Steric-model for activation of muscle thin filaments. *J. Mol. Biol.* **266**, 8-14
11. Ishikawa, T. and Wakabayashi, T. (1994) Calcium induced change in three-dimensional structure of thin filaments of rabbit skeletal muscle as revealed by cryo-electron microscopy. *Biochem. Biophys. Res. Commun.* **203**, 951-958
12. Ishikawa, T. and Wakabayashi, T. (1995) Proposal of alignment-independent classification of electron microscopic images with helical symmetry and its application to reconstituted thin filaments of skeletal muscle. *Ultramicroscopy* **57**, 91-101
13. Seymour, J. and O'Brien, E.J. (1980) The position of tropomyosin in muscle thin filaments. *Nature* **283**, 680-682
14. Kabsch, W. and Vandekerckhove, J. (1992) Structure and function of actin. *Annu. Rev. Biophys. Biomol.* **21**, 49-76
15. Poole, K.J.V., Lorenz, M., Evans, G., Rosenbaum, G., and Holmes, K.C. (1994) The effect of calcium on the regulated thin filament structure. *Biophys. J.* **66**, A347
16. Kabsch, W., Mannherz, H.G., Suck, D., Pai, E.F., and Holmes, K.C. (1990) Atomic structure of the actin: DNaseI complex. *Nature* **347**, 37-44
17. Miki, M., Kobayashi, T., Kimura, H., Hagiwara, A., Hai, H., and Maéda, Y. (1998) Ca^{2+}-induced distance change between points on actin and troponin in skeletal muscle thin filaments estimated by fluorescence energy transfer spectroscopy. *J. Biochem.* **123**, 324-331
18. Popp, D. and Maéda, Y. (1993) Calcium ions and the structure of muscle actin filament: an X-ray diffraction study. *J. Mol. Biol.* **229**, 279-285
19. Borovikov, Y.S., Nowak, E., Khoroshev, M.I., and Dąbrowska, R. (1993) The effect of Ca^{2+} on the conformation of tropomyosin and actin in regulated actin filaments with or without bound myosin subfragment 1. *Biochim. Biophys. Acta* **1163**, 280-286
20. Wakabayashi, K., Tanaka, H., Saito, H., Moriwaki, N., Ueno, Y., and Amemiya, Y. (1991) Dynamic X-ray diffraction of skeletal muscle contraction: structural change of actin filaments. *Adv. Biophys.* **27**, 3-13
21. Wakabayashi, K., Ueno, Y., Amemiya, Y., and Tanaka, H. (1988) Intensity changes of actin-based layer lines from frog skeletal muscles during an isometric contraction in *Molecular Mechanism of Muscle Contraction* (Sugi, H. and Pollack, G.H., eds.) pp. 353-367, Plenum Press, New York and London
22. Al-Khayat, H.A., Yagi, N., and Squire, J.M. (1995) Structural changes in actin-tropomyosin during muscle regulation: computer modelling of low-angle X-ray diffraction data. *J. Mol. Biol.* **252**, 611-632
23. Squire, J.M. and Morris, E.P. (1998) A new look at thin filament regulation in vertebrate skeletal muscle. *FASEB J.* **12**, 761-771
24. Ebashi, S., Ebashi, F., and Kodama, A. (1967) Troponin as the Ca^{++}-receptive protein in the contractile system. *J. Biochem.* **62**, 137-138
25. Greene, L.E. and Eisenberg, E. (1980) Cooperative binding of myosin subfragment-1 to the actin-troponin-tropomyosin complex. *Proc. Natl. Acad. Sci. USA* **77**, 2616-2620
26. Hill, T.L., Eisenberg, E., and Greene, L.E. (1980) Theoretical model for the cooperative equilibrium binding of myosin subfragment 1 to the actin-troponin-tropomyosin complex. *Proc. Natl. Acad. Sci. USA* **77**, 3186-3190
27. Nagashima, H. and Asakura, S. (1980) Dark-field light microscopic study of the flexibility of F-actin complexes. *J. Mol. Biol.* **136**, 169-182
28. Geeves, M.A. and Halsall, D.J. (1987) Two-step ligand binding and cooperativity. *Biophys. J.* **52**, 215-220
29. Yagi, N. and Matsubara, I. (1989) Structural changes in the thin filament during activation studied by X-ray diffraction of highly stretched skeletal muscle. *J. Mol. Biol.* **208**, 359-363
30. Lehrer, S.S. and Morris, E.P. (1982) Dual effects of tropomyosin and troponin-tropomyosin on actomyosin subfragment 1 ATPase. *J. Biol. Chem.* **257**, 8073-8080
31. Lehrer, S.S. and Geeves, M.A. (1998) The muscle thin filaments as a classical cooperative/allosteric regulatory system. *J. Mol. Biol.* **277**, 1081-1089
32. Perutz, M.F. (1989) Mechanisms of cooperativity and allosteric regulation in proteins. *Q. Rev. Biophys.* **22**, 139-236
33. Maytum, R., Lehrer, S.S., and Geeves, M.A. (1999) Cooperactivity and switching within the three-state model of muscle regulation. *Biochemistry* **38**, 1102-1110
34. Tao, T., Gong, B.-J., and Leavis, P.C. (1990) Calcium-induced movement of troponin-I relative to actin in skeletal muscle thin filaments. *Science* **247**, 1339-1341
35. Miki, M. and Iio, T. (1993) Kinetics of structural changes of reconstituted skeletal muscle thin filaments observed by fluorescence resonance energy transfer. *J. Biol. Chem.* **268**, 7101-7106
36. Lehrer, S.S. (1994) The regulatory switch of the muscle thin filament: Ca^{2+} or myosin heads? *J. Muscle Res. Cell Motil.* **15**, 232-236
37. Saeki, K., Sutoh, K., and Wakabayashi, T. (1996) Tropomyosin-binding site(s) on the *Dictyostelium* actin surface as identified by site-directed mutagenesis. *Biochemistry* **35**, 14465-14472
38. Herzberg, O. and James, M.N.G. (1988) Refined crystal structure of troponin C from turkey skeletal muscle at 2.0 Å resolution. *J. Mol. Biol.* **203**, 761-779
39. Slupsky, C.M. and Sykes, B.D. (1995) NMR solution structure of calcium-saturated skeletal muscle troponin C. *Biochemistry* **34**, 15953-15964
40. Gagné, S.M., Tsuda, S., Li, M.X., Smillie, L.B., and Sykes, B.D. (1995) Structures of the troponin C regulatory domains in the apo and calcium-saturated states. *Nat. Struct. Biol.* **2**, 784-789
41. Houdusse, A., Love, M.L., Dominguez, R., Grabarek, Z., and Cohen, C. (1997) Structures of four Ca^{2+}-bound troponin C at 2.0 A resolution: further insights into the Ca^{2+}-switch in the calmodulin superfamily. *Structure* **5**, 1695-1711
42. Vassylyev, D.G., Takeda, S., Wakatsuki, S., Maeda, K., and Maéda, Y. (1998) Crystal-structure of troponin C in complex with troponin I fragment at 2.3-Å resolution. *Proc. Natl. Acad. Sci. USA* **95**, 4847-4852
43. Farah, C.S., Miyamoto, C.A., Ramos, C.H.I., da Silva, A.C.R.,

Quaggio, R.B., Fujimori, K., Smillie, L.B., and Reinach, F.C. (1994) Structural and regulatory functions of the NH_2- and COOH-terminal regions of skeletal muscle troponin I. *J. Biol. Chem.* **269**, 5230-5240
44. Tao, T., Gowell, E., Strasburg, G.M., Gergely, J., and Leavis, P.C. (1989) Ca^{2+} dependence of the distance between Cys-98 of troponin C and Cys-133 of troponin I in the ternary troponin complex. Resonance energy transfer measurements. *Biochemistry* **28**, 5902-5908
45. Hodgkinson, J.L., EL-Mezgueldi, M., Craig, R., Vibert, P., Marston, S.B., and Lehman, W. (1997) 3-D image reconstruction of reconstituted smooth muscle thin filaments containing calponin: visualization of interactions between F-actin and calponin. *J. Mol. Biol.* **273**, 150-159
46. Lehman, W., Vibert, P., and Craig, R. (1997) Visualization of caldesmon on smooth muscle thin filaments. *J. Mol. Biol.* **274**, 310-317
47. Owen, C. and DeRosier, D. (1993) A 13-Å map of the actin-scruin filament from the Limulus acrosomal process. *J. Cell Biol.* **123**, 337-344
48. McGough, A., Way, M., and DeRosier, D. (1994) Determination of the α-actinin-binding site on actin filaments by cryoelectron microscopy and image analysis. *J. Cell Biol.* **126**, 433-443
49. Hanein, D., Matsudaira, P., and DeRosier, D.J. (1997) Evidence for a conformational change in actin induced by fimbrin (N375) binding. *J. Cell Biol.* **139**, 387-396
50. Ohtsuki, I. and Wakabayashi, T. (1972) Optical diffraction studies on the structure of troponin-tropomyosin-actin paracrystals. *J. Biochem.* **72**, 369-377
51. Ebashi, S., Wakabayashi, T., and Ebashi, F. (1971) Troponin and its components. *J. Biochem.* **69**, 441-445
52. Spudich, J.A. and Watt, S. (1971) The regulation of rabbit skeletal muscle contraction. *J. Biol. Chem.* **246**, 4866-4871
53. Laemmli, U.K. (1970) Cleavage of structural proteins during the assembly of the head of bacteriophage T4. *Nature* **227**, 680-685
54. Dubochet, J., Adrian, M., Chang, J.-J., Homo, J.-C., Lepault, J., McDowall, A.W., and Schultz, P. (1988) Cryo-electron microscopy of vitrified specimens. *Q. Rev. Biophys.* **21**, 129-228
55. Egelman, E.H. (1986) An algorithm for straightening images of curved filamentous structures. *Ultramicroscopy* **19**, 367-374
56. DeRosier, D.J. and Moore, P.B. (1970) Reconstruction of three-dimensional images from electron micrographs of structures with helical symmetry. *J. Mol. Biol.* **52**, 355-369
57. Crowther, R.A., Henderson, R., and Smith, A. (1996) MRC image processing programs. *J. Struct. Biol.* **116**, 9-16
58. Potter, J.D. and Gergely, J. (1974) Troponin, tropomyosin, and actin interactions in the Ca^{2+} regulation of muscle contraction. *Biochemistry* **13**, 2697-2703
59. Ueno, Y., Moriwaki, N., and Wakabayashi, K. (1994) Modelling structural changes of the muscle thin filaments during an isomeric contraction in *Synchrotron Radiation in the Biosciences* (Chance, B. *et al.*, eds.) pp. 443-450, Clarendon Press, New York
60. Holmes, K.C., Popp, D., Gebhard, W., and Kabsch, W. (1990) Atomic model of the actin filament. *Nature* **347**, 44-49
61. Rayment, I., Holden, H.M., Whittaker, M., Yohn, C.B., Lorenz, M., Holmes, K.C., and Milligan, R.A. (1993) Structure of the actin-myosin complex and its implications for muscle contraction. *Science* **261**, 58-65
62. Makuch, R., Kotakowski, J., and Dąbrowska, R. (1992) The importance of C-terminal amino acid residues of actin to the inhibition of actomyosin ATPase activity by caldesmon and troponin I. *FEBS Lett.* **297**, 237-240
63. Luo, Y., Wu, J.-L., Gergely, J., and Tao, T. (1997) Troponin T and Ca^{2+} dependence of the distance between Cys48 and Cys133 of troponin I in the ternary troponin complex and reconstituted thin filaments. *Biochemistry* **36**, 11027-11035
64. Tripet, B., Van Eyk, J.E., and Hodges, R.S. (1997) Mapping of a second actin-tropomyosin and a second troponin C binding site within the C terminus of troponin I, and their importance in the Ca^{2+}-dependent regulation of muscle contraction. *J. Mol. Biol.* **271**, 728-750
65. Olah, G.A. and Trewhella, J. (1994) A model structure of the muscle protein complex $4Ca^{2+}$-troponin C-troponin I derived from small-angle scattering data: implications for regulation. *Biochemistry* **33**, 12800-12806
66. Sheeham, B., Fuller, S.D., Pique, M.E., and Yeager, M. (1996) AVS software for visualization in molecular microscopy. *J. Struct. Biol.* **116**, 99-106